PHYSICAL REVIEW A **70**, 011402(R) (2004)

Photodetachment in a strong circularly polarized laser field

Svea Beiser, Michael Klaiber, and Igor Yu. Kiyan
Physikalisches Institut, Albert-Ludwigs-Universität, D-79104 Freiburg, Germany
(Received 23 January 2004; published 21 July 2004)

The saddle-point analysis of the transition amplitude shows that the quantum interference effect does not occur in the direct process of photodetachment by a circularly polarized laser field. This fact is interpreted in terms of classical electron trajectories. Comparison between the length and velocity gauges is performed by simulating spectra of photoelectrons produced in a focus of a laser pulse. A substantial discrepancy is found in the kinetic energy distribution of photoelectrons. At low energies, only the predictions in the length gauge are consistent with the Wigner threshold law.

DOI: 10.1103/PhysRevA.70.011402 PACS number(s): 32.80.Rm, 32.80.Gc

Ionization of an atomic system in a strong laser field received great interest during past decades. Numerous nonperturbative methods have been developed to treat the problem. Among these are the Keldysh-Faisal-Reiss (KFR) theory [1–3] and its various modifications [4,5], the *R*-matrix Floquet theory [6–8], the Floquet close-coupling method [9], the non-Hermitian Floquet Hamiltonian method [10], the quasistationary quasienergy states (QQES) approach [11], and direct numerical integration methods [12,13].

The analytical KFR theory is a most fascinating approach. Despite to the fact that it was first proposed by Keldysh 40 years ago and since that time has been under intensive discussion, a deeper analysis of its results still continues to give insight into the physics of photoionization. A great advantage of the KFR theory is its analyticity. It enables us to describe the phenomenon of ionization on a more fundamental level, relating it to a coherent superposition of electron trajectories in the continuum. In particular, the effect of quantum interference in the direct process of ionization is intrinsically included in the final expression describing the ionization rate. Only recently this matter came into discussion, after experiments on strong-field photodetachment of negative ions in a linearly polarized laser field revealed an interference structure in photoelectron spectra [14,15].

Theoretically, the interference effect arises due to a superposition of saddle-point contributions in the complex time plane. Within the oscillation period of a linearly polarized field, there are two such points contributing to the amplitude of electron emission with a given momentum vector. The saddle points are attributed to two spatially separated electron emitters aligned along the polarization axis of the field. Such a semiclassical description of ionization reflects the fact that in a harmonic field, the bound electron can be released at either side from the core along the external force direction. The two emitters are coherent, and thus, their superposition gives rise to the interference structure in the angle-resolved momentum distribution of photoelectrons. In the limit of small photoelectron momenta the effect reduces to a simple picture of a two-slit interference [14,16]. Quantum interference is not restricted, however, to low kinetic energies, rather this effect is ubiquitous in the emission spectrum of photoelectrons [15].

The quantum interference effect is also predicted by the QQES method [11] and by non-perturbative Floquet method [17]. Their results are in accord with the KFR theory and with the recent experimental observations. Developed to describe photodetachment from a short-range potential, the QQES method provides an exact solution for the detachment rate [18]. Though the direct relation of results by this method to the quantum interference effect is masked by the numerical routine, it does predict the interference structure similar to the one predicted by the Keldysh-like theory.

To date, the quantum interference has been considered only for the case of linearly polarized laser field. In the present work we investigate its role in the process of ionization by a circularly polarized field. Our approach is analogous to the one developed by Gribakin and Kuchiev [4], and it employs the saddle-point analysis of contributions to the multiphoton transition amplitude. The method is based on the strong field approximation, which neglects the core potential in the description of the final electron state. This approximation is justified when the electron is initially bound by short-range forces. Thus, the method is suited for the description of the process of photodetachment of negative ions, where the asymptotic Coulomb potential of the core is absent. In our calculations we use the length gauge to describe the field interaction. Though the velocity gauge simplifies the consideration for circular polarization [3], it was argued, however, that the length gauge should be used to obtain correct results for the photodetachment rate [4]. We show below that the two approaches substantially differ in their predictions. We also discuss the origin of this difference and provide a judgment on the proper gauge to use in the KFR theory.

Let us consider the process of photodetachment in a circularly polarized laser field $\mathbf{F}(t)=F\mathbf{(}\cos(\omega t),\sin(\omega t),0\mathbf{)}$, where F and ω are the field strength and frequency, respectively. The polarization plane is assumed to coincide with the (x,y) coordinate plane and the polarization direction is counterclockwise. Following the adiabatic approximation of Gribakin and Kuchiev [4], the n-photon differential detachment rate has the form (atomic units $\hbar=e=m_e=1$ are used throughout)

$$dw_n = 2\pi|A_{\mathbf{p}n}|^2\delta\left(\frac{p^2}{2}+\frac{F^2}{2\omega^2}-E_0-n\omega\right)\frac{d^3p}{(2\pi)^3}. \qquad (1)$$

Here $E_0=-\kappa^2/2$ is the energy of the initial bound state, $\mathbf{p}$ is the momentum of the outgoing electron, and $A_{\mathbf{p}n}$ represents

the amplitude of the transition to the final state. The energy of the final state is determined by the energy conservation rule represented by the δ function in Eq. (1), where the term $F^2/2\omega^2$ corresponds to the ponderomotive shift of the detachment threshold. Neglecting the core potential in the description of the final state, the wave function of the outgoing electron is represented by the Volkov function. In the length gauge, the transition amplitude acquires the form

$$A_{\mathbf{p}n} = \frac{\omega}{2\pi}\int_0^{2\pi/\omega}\left(E_0 - \frac{(\mathbf{p}+\mathbf{k}_t)^2}{2}\right)\tilde{\phi}_0(\mathbf{p}+\mathbf{k}_t) \times \exp\left\{\frac{i}{2}\int^t [(\mathbf{p}+\mathbf{k}_{t'})^2 - 2E_0]dt'\right\}dt, \qquad (2)$$

where $\mathbf{k}_t = \int^t dt' \mathbf{F}(t')$ is the classical electron momentum due to the field and $\tilde{\phi}_0(\mathbf{q})$ is the Fourier transform of the initial electron wave function. More details on derivation of Eq. (2) can be found in Ref. [4].

The integrand function of Eq. (2) contains a rapidly oscillating exponent $\exp[iS(\omega t)]$, where $S(\omega t)$ represents the coordinate-independent classical action. Thus, the integral over time can be calculated analytically by using the method of steepest descents. In the case of circularly polarized field, the explicit form of the action is

$$S(\omega t) = n\omega t - \frac{F}{\omega^2}p_\parallel \cos(\omega t - \varphi), \qquad (3)$$

where $p_\parallel = p\cos\theta$ is the component of the momentum $\mathbf{p}$ parallel to the polarization plane, θ is the angle of electron emission with respect to the polarization plane, and $\varphi = \arccos(p_x/p_\parallel)$ represents the azimuthal angle in this plane. The saddle-point condition is defined by $S'(\omega t_s) = 0$ and has a pair of complex conjugate roots. According to the theory of adiabatic transitions, only the root with a positive imaginary part is of physical meaning. It has the following form

$$\omega t_s = \frac{3}{2}\pi + \varphi + i\ln\left(\frac{n\omega^2}{Fp_\parallel} + \sqrt{\frac{n^2\omega^4}{F^2p_\parallel^2} - 1}\right). \qquad (4)$$

Thus, only one saddle point contributes to the transition amplitude. This is in contrast to the case of linearly polarized laser field, where contributions from two saddle points define a coherent superposition of two emitted matter waves, giving rise to an interference pattern in the photoelectron spectrum. The quantum interference in the process of photodetachment by circularly polarized field does not exist. This fact can be illustrated by considering classical electron trajectories. Disregarding the core potential, the electron in a circularly polarized field moves on a circular orbit established during the adiabatic switching on the field. In this adiabatic case, the coordinate phase of the circular motion in the (x,y) polarization plane matches the rotational phase of the field strength vector. The instant of electron emission with a given momentum $\mathbf{p}$ is determined by the saddle point t_s. It should be understood that the real part of the complex time t_s corresponds to the real time scale. It follows from Eq. (4) that the electron emission at a given azimuthal angle φ occurs when the phase associated with the circular motion acquires the value $\varphi + 3\pi/2$. This value corresponds to the tangential emission from the orbit, as depicted in Fig. 1(a). The origin of the tangential trajectory is uniquely defined by the emission angle, and no such trajectories that are parallel or that intersect each other exist. Therefore, the interference effect is absent.

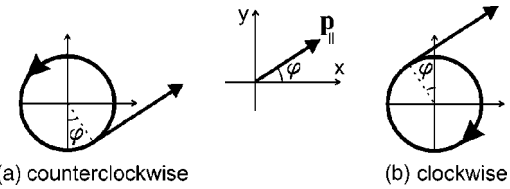

FIG. 1. Electron emission from a circular orbit at the azimuthal angle φ in the plane of circular polarization. (a) and (b) show tangential trajectories of the ejected electron for the counterclockwise and clockwise polarization of the field, respectively. Origins of these trajectories are located at opposite sides from the core.

It is easy to perform similar calculations for a clockwise circularly polarized field. In this case the electron is released when the phase of circular motion is $\varphi - 3\pi/2$, which also results in the tangential emission [Fig. 1(b)]. The classical consideration of electron trajectories provides a simple qualitative interpretation of the interference effect in photodetachment by a linearly polarized field. Linear polarization can be represented by a superposition of clockwise and counterclockwise circular polarizations. Consequently, the electron emission into a given angle undergoes two paths, corresponding to the two different trajectories shown in Fig. 1. A coherent superposition of these paths, as appropriate for linear polarization, gives rise to interference analogous to two-slit interference.

The rest of the calculations represent a straightforward routine. As it was discussed in [4], in the length gauge the transition amplitude is determined by the contribution from large distances. Then, it is sufficient to describe the initial state by its asymptotic wave function. For a negative ion it has the form $\phi_0(\mathbf{r}) = Ar^{-1}\exp(-\kappa r)Y_{lm}(\hat{\mathbf{r}})$, where A is the normalization coefficient, Y_{lm} is a spherical harmonic, and l,m are the angular momentum quantum numbers of the electron in the initial state. The quantization axis of the angular momentum coincides with the z axis. The Fourier transform of ϕ_0 calculated at the saddle point is given by $\tilde{\phi}_0(\mathbf{q}) = 4\pi A(q^2+\kappa^2)^{-1}Y_{lm}(\hat{\mathbf{q}})$, where $q \to i\kappa$, and the argument of Y_{lm} is a complex vector. The complex spherical angles $\theta_\mathbf{q}, \varphi_\mathbf{q}$ can be expressed by using a formal definition: $\cos\theta_\mathbf{q} = \mathbf{q}\cdot\hat{\mathbf{z}}/\sqrt{\mathbf{q}^2}$, $\cos\varphi_\mathbf{q} = \mathbf{q}_\parallel\cdot\hat{\mathbf{x}}/\sqrt{\mathbf{q}_\parallel^2}$, where $\mathbf{q}_\parallel = \mathbf{p}_\parallel + \mathbf{k}_{t_s}$ is the component of the complex momentum $\mathbf{q}$ parallel to the polarization plane. Evaluating the integrand of Eq. (2) at the saddle point, substituting $A_{\mathbf{p}n}$ into Eq. (1), and integrating the latter over the coordinate p of the momentum space, for the differential n-photon detachment rate we obtain

$$\frac{dw_n}{d\Omega} = \frac{A^2\omega^2}{8\pi^2}(2l+1)\frac{(l-|m|)!}{(l+|m|)!}\left|P_l^{|m|}\left(i\frac{p}{\kappa}\sin\theta\right)\right|^2 \times \frac{(\eta - \sqrt{\eta^2-1})^{2n}}{\sqrt{\eta^2-1}F\cos\theta}\left[\frac{\sqrt{\kappa^2 + p^2\sin^2\theta}}{\frac{F}{\omega}(\eta + \sqrt{\eta^2-1}) - p\cos\theta}\right]^{2m} \times \exp[2Fp\cos\theta\sqrt{\eta^2-1}/\omega^2], \qquad (5)$$

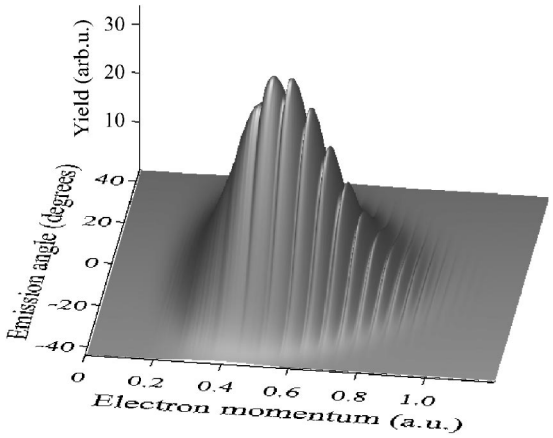

FIG. 2. The spectrum of photoelectrons produced by photodetachment of F^- in a laser pulse of 1400 nm wavelength and 2×10^{13} W/cm^2 peak intensity.

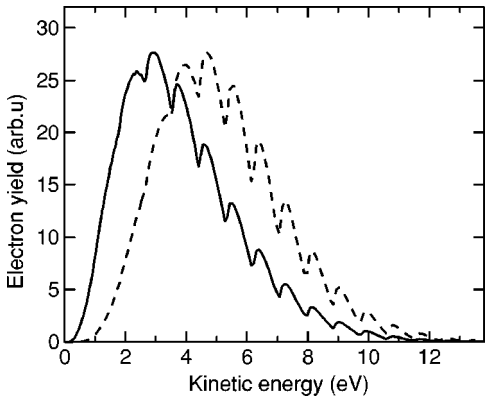

FIG. 3. Electron distribution over the kinetic energy in the plane of circular polarization. Solid and dashed curves correspond to predictions in the length and in the velocity gauge, respectively. The curves are normalized to each other at the maximum yield.

where $\eta=n\omega^2/(Fp\cos\theta)$, $P_l^{|m|}(Z)$ is the Legendre polynomial, and $p=(2n\omega-F^2/\omega^2+2E_0)^{1/2}$ is the electron momentum determined by the energy conservation rule.

Equation (5) is used to simulate a spectrum of photoelectrons produced by photodetachment in a laser pulse of high intensity. The simulation is performed for realistic experimental conditions where F^- ions interact with a focused laser beam of 1400 nm wavelength and $I_0=2\times10^{13}$ W/cm^2 peak intensity. The initial p state ($l=1$) of F^- has the binding energy $E_0=-3.401\,188\,7$ eV [19]. The calculation routine is analogous to the one described in Ref. [15]. It involves summation of photodetachment rates for different values $m=0,\pm1$ of the projection of the initial angular momentum, the statistical averaging of detachment channels associated with the two spin-orbit sublevels, $^2P^o_{1/2}$ and $P^o_{3/2}$, of the final atomic state, and integration of the electron yield over the intensity distribution in the laser focus. The result of simulation is presented in Fig. 2. The figure shows the electron distribution over the momentum scale and the emission angle with respect to the plane of circular polarization. The spectrum consists of contributions from a series of excess photon detachment peaks with $n\geqslant4$. The peaks are ponderomotively shifted and broadened and overlapping each other, giving rise to the regular structure along the momentum axis. The spectrum, however, does not exhibit any structure associated with the quantum interference effect.

In the following we compare these results with predictions obtained by using the velocity gauge. The differential n-photon detachment rate in the velocity gauge has the form [3]

$$\frac{dw_n}{d\Omega}=\frac{\omega^2 p}{(2\pi)^2}\left(n-\frac{F^2}{2\omega^3}\right)^2|\tilde{\phi}_0(\mathbf{p})|^2J_n^2\left(\frac{n}{\eta}\right), \tag{6}$$

where η is introduced in Eq. (5), J_n is the Bessel function, and $\tilde{\phi}_0(\mathbf{p})$ is the Fourier transform of the initial wave function calculated at the momentum $\mathbf{p}$ of the outgoing electron. The presentation of the initial wave function by its asymptotic form is not justified in the velocity gauge. Therefore, here we use the Hartree-Fock wave function of the valence electron in F^-. This function is given in Ref. [20] in a parametrized analytical form, and its Fourier transform can be calculated analytically

$$\tilde{\phi}_0(\mathbf{p})=-32\pi iY_{1m}(\hat{\mathbf{p}})\sum_{i=1}^{4}C_iN_i\frac{\xi_i p}{(p^2+\xi_i^2)^3}, \tag{7}$$

where numerical parameters C_i, N_i, ξ_i are given in [20].

Equations (6) and (7) are used in a simulation of the photoelectron spectrum of F^- at the same laser parameters as described above. The shape of the spectrum is similar to the one shown in Fig. 2. For a quantitative comparison, we present in Fig. 3 the kinetic energy distribution of electrons emitted in the plane of circular polarization. The solid and dashed curves correspond to calculations in the length and in the velocity gauge, respectively. The figure shows a substantial discrepancy between the two predictions. In particular, the relative yield of electrons with low kinetic energies is considerably enhanced in the length gauge compared to the velocity gauge. The maxima of the two distributions appear at different kinetic energies, separated by approximately twice the photon energy. Such a difference can be easily resolved experimentally.

The discrepancy found here arises from the fact that the photodetachment rate in the length gauge is dependent on the value m of the projection of the initial angular momentum [see Eq. (5)]. In contrast, predictions in the velocity gauge are dependent on its absolute value $|m|$. In order to explore this fact deeper, let us consider the threshold limit $p\to0$. In this limit the detachment process should obey the Wigner threshold law [21]. Its validity under strong laser field conditions has been discussed in Ref. [22]. The law predicts the detachment rate to be proportional to $p^{2\ell_f+1}$, where ℓ_f is the angular momentum of the electron in the final continuum state. In the case of F^- considered here ($l=1, n\geqslant4$), the lowest final-state angular momentum according to the selection rules is $\ell_f=n-1$ for the initial state with $m=-1$, and $\ell_f=n+1$ for $m=0,+1$. Expanding Eq. (5) over p in the limit of low momenta and taking the first significant term into account, we find that the n-photon detachment rate is propor-

tional to $p^{2(n-1)+1}$ when $m=-1$, and it is proportional to $p^{2(n+1)+1}$ when $m=0,+1$. This result is absolutely consistent with the Wigner law [23]. In contrast, predictions in the velocity gauge fail to reproduce the threshold law. Indeed, expanding Eqs. (6) and (7) in the limit $p\rightarrow 0$, we find that the detachment rate is proportional to $p^{2(n+1)+1}$, independent on the value m of the projection of the initial angular momentum. As a consequence, the detachment yield near threshold from the $m=-1$ initial state is lower in the velocity gauge. For example, in the lowest order detachment channel considered here, $n=4$, it is proportional to p^{11} instead of p^7. This explains the discrepancy at low kinetic energies shown in Fig. 3.

In conclusion, it has been shown that the quantum interference effect is absent in photodetachment by circularly polarized laser radiation. A substantial and experimentally observable discrepancy is found between kinetic energy distributions of photoelectrons calculated in the length and in the velocity gauge, respectively. The discrepancy arises from the fundamentally different character of contributions from initial states with positive and negative values of the angular momentum quantum number m, as predicted in this work. In the limit of low electron energies, only the calculations in the length gauge are consistent with the Wigner threshold law. Thus, the length gauge is proper to use in the Keldysh approximation. This result represents an important cornerstone in the years-long discussion on the appropriate gauge to use in the KFR theory.

The authors greatly appreciate fruitful discussions of this work with Professor Hanspeter Helm. This research was supported by the Deutsche Forschungsgemeinschaft, Grant No. KI 865/1-1.

[1] L.V. Keldysh, Sov. Phys. JETP **20**, 1307 (1964).
[2] F.H.M. Faisal, J. Phys. B **6** L89 (1973).
[3] H.R. Reiss, Phys. Rev. A **22**, 1786 (1980).
[4] G.F. Gribakin and M.Yu. Kuchiev, Phys. Rev. A **55**, 3760 (1997).
[5] A. Lohr *et al.*, Phys. Rev. A **55** R4003 (1997).
[6] P.G. Burke, P. Francken, and C.J. Joachain, Europhys. Lett. **13**, 617 (1990); J. Phys. B **24**, 761 (1991).
[7] M. Dörr *et al.*, J. Phys. B **28**, 4481 (1995).
[8] H.W. van der Hart, J. Phys. B **29**, 3059 (1996).
[9] L. Dimou and F.H.M. Faisal, J. Phys. B **27**, L333 (1994).
[10] D.A. Telnov and S.I. Chu, Phys. Rev. A **59**, 2864 (1999).
[11] B. Borca *et al.*, Phys. Rev. Lett. **87**, 133001 (2001).
[12] H.G. Muller and F.C. Kooiman, Phys. Rev. Lett. **81**, 1207 (1998).
[13] R. Wiehle *et al.*, Phys. Rev. A **67**, 063405 (2003).
[14] R. Reichle, H. Helm, and I.Yu. Kiyan, Phys. Rev. Lett. **87**, 243001 (2001).
[15] I.Yu. Kiyan and H. Helm, Phys. Rev. Lett. **90**, 183001 (2003).
[16] R. Reichle, I.Yu. Kiyan, and H. Helm, J. Mod. Opt. **50**, 461 (2003).
[17] D.A. Telnov and S.I. Chu, Phys. Rev. A **66**, 063409 (2002).
[18] M.V. Frolov *et al.*, Phys. Rev. Lett. **91**, 053003 (2003).
[19] T. Andersen, H.K. Haugen, and H. Hotop, J. Phys. Chem. Ref. Data **28**, 1511 (1999).
[20] A.A. Radzig and B.M. Smirnov, *Reference Data on Atoms, Molecules, and Ions* (Springer, Berlin, 1985).
[21] E.P. Wigner, Phys. Rev. **73**, 1002 (1948).
[22] R. Reichle, H. Helm, and I.Yu. Kiyan, Phys. Rev. A **68**, 063404 (2003).
[23] The Wigner law can be easily derived from Eq. (5) in a general case of arbitrary values of n and l, provided that $n \geqslant l$. Since the Keldysh approximation assumes $n \gg 1$, this condition is satisfied.